

# Functional Profiling Identifies Determinants of Arsenic Trioxide Cellular Toxicity

Amin Sobh,<sup>\*,†</sup> Alex Loguinov,<sup>\*</sup> Gulce Naz Yazici,<sup>\*,‡</sup> Rola S. Zeidan,<sup>\*</sup> Abderrahmane Tagmount,<sup>\*</sup> Nima S. Hejazi,<sup>§,¶</sup> Alan E. Hubbard,<sup>§</sup> Luoping Zhang,<sup>||</sup> and Chris D. Vulpe<sup>\*,†,1</sup>

<sup>\*</sup>Department of Physiological Sciences, College of Veterinary Medicine, University of Florida, Gainesville, Florida; <sup>†</sup>Department of Nutritional Sciences & Toxicology, Comparative Biochemistry Program, University of California, Berkeley, Berkeley, California; <sup>‡</sup>Department of Histology and Embryology, Faculty of Medicine, Erzincan Binali Yildirim University, Erzincan, Turkey; <sup>§</sup>Division of Biostatistics and Epidemiology, School of Public Health; <sup>¶</sup>Center for Computational Biology; and <sup>||</sup>Division of Environmental Health Sciences, School of Public Health, University of California, Berkeley, Berkeley, California

<sup>1</sup>To whom correspondence should be addressed at Department of Physiological Sciences, University of Florida, Gainesville, Center for Environmental and Human Toxicology, 187 Mowry Drive, Building 471, PO Box 110885, Gainesville, FL 32611. Fax: 352-392-2938; E-mail: cvulpe@ufl.edu.

## ABSTRACT

Arsenic exposure is a worldwide health concern associated with an increased risk of skin, lung, and bladder cancer but arsenic trioxide (As<sup>III</sup>) is also an effective chemotherapeutic agent. The current use of As<sup>III</sup> in chemotherapy is limited to acute promyelocytic leukemia (APL). However, As<sup>III</sup> was suggested as a potential therapy for other cancer types including chronic myeloid leukemia (CML), especially when combined with other drugs. Here, we carried out a genome-wide CRISPR-based approach to identify modulators of As<sup>III</sup> toxicity in K562, a human CML cell line. We found that disruption of KEAP1, the inhibitory partner of the key antioxidant transcription factor Nrf2, or TXNDC17, a thioredoxin-like protein, markedly increased As<sup>III</sup> tolerance. Loss of the water channel AQP3, the zinc transporter ZNT1 and its regulator MTF1 also enhanced tolerance to As<sup>III</sup> whereas loss of the multidrug resistance protein ABCC1 increased sensitivity to As<sup>III</sup>. Remarkably, disruption of any of multiple genes, *EEFSEC*, *SECISBP2*, *SEPHS2*, *SEPSECS*, and *PSTK*, encoding proteins involved in selenocysteine metabolism increased resistance to As<sup>III</sup>. Our data suggest a model in which an intracellular interaction between selenium and As<sup>III</sup> may impact intracellular As<sup>III</sup> levels and toxicity. Together this work revealed a suite of cellular components/processes which modulate the toxicity of As<sup>III</sup> in CML cells. Targeting such processes simultaneously with As<sup>III</sup> treatment could potentiate As<sup>III</sup> in CML therapy.

**Key words:** arsenic; selenium; CRISPR screen; selenocysteine.

Arsenic toxicity is a worldwide public health concern as millions of people are exposed to this metalloid in drinking water (Ravenscroft, 2007) at levels above the 10 µg/l guideline of the World Health Organization (WHO, 1996). In the United States, arsenic is ranked first in the Priority List of Hazardous Substances (ATSDR, 2017). Acute arsenic poisoning can result in severe digestive and neurologic effects and ultimately death while chronic arsenic exposure increases the risk of skin, lung, and bladder cancers (IARC, 2004; Ratnaik, 2003). However,

arsenic trioxide (As<sub>2</sub>O<sub>3</sub>/ATO; As<sup>III</sup>) has been historically used as a traditional Chinese medicine and was found to be a highly effective treatment of acute promyelocytic leukemia (APL) (Mathews et al., 2006, 2010; Shen et al., 1997; Zhou et al., 2010). In combination with all-trans retinoic acid, As<sup>III</sup> results in remission rates approaching 96% in APL patients (Abaza et al., 2017; Lo-Coco et al., 2016). The major therapeutic effect of As<sup>III</sup> involves degradation of the fusion oncoprotein promyelocytic leukemia (PML)-retinoic acid receptor-α (RARα) (Zhang et al.,

2010) and subsequent induction of partial differentiation and apoptosis in APL cells (Emadi and Gore, 2010). As<sup>III</sup>-induced cytotoxic effects that are independent of PML-RAR $\alpha$  degradation also exist in APL cells and likely contribute to the observed substantial efficacy of As<sup>III</sup> (Davison et al., 2002; Yedjou et al., 2010).

Despite its exclusive use in APL therapy, As<sup>III</sup> demonstrated a promising therapeutic potential in multiple types of hematologic malignancies (Berenson et al., 2006; Kchour et al., 2009; Wang et al., 2015; Zheng et al., 2008). The cytotoxic effects of As<sup>III</sup> have been studied in various non-APL cancer cells (Akao et al., 1999; Rousselot et al., 1999; Shen et al., 1999; Zhang et al., 1998). The mechanisms of As<sup>III</sup> toxicity remain unclear although a variety of mechanisms that likely vary depending on the cell type have been proposed (Miller et al., 2002). Inside the cell, inorganic As<sup>III</sup> (iAs<sup>III</sup>) is typically metabolized to methylated forms including monomethylarsonic acid (MMA<sup>V</sup>), dimethylarsenic acid (DMA<sup>V</sup>), monomethylarsonous acid (MMA<sup>III</sup>), and dimethylarsinous acid (DMA<sup>III</sup>) (Hopenhayn-Rich et al., 1993; Vahter, 2002). MMA<sup>III</sup> is likely the primary toxic species (Mass et al., 2001; Styblo et al., 2002) although the other forms may have direct effects. Cytotoxic effects of As<sup>III</sup> are mainly exerted through its reaction with the thiol groups of a variety of intracellular proteins (Watson, 2015) and the diversity of As<sup>III</sup> targets likely underlies the complex nature of its toxicity.

In this study, we employed a genome-wide CRISPR/Cas9 loss-of-function screen to identify genes whose disruption alters sensitivity to As<sup>III</sup> in the erythroleukemic K562 cell line which does not contain the PML-RAR $\alpha$  rearrangement. Our study thus focuses on cellular mechanisms of As<sup>III</sup> toxicity independent of PML-RAR $\alpha$  degradation. We confirmed the existing pathways that are involved in As<sup>III</sup> toxicity and identified novel pathways that influence sensitivity to As<sup>III</sup>. This work provided new insights into the molecular mechanisms which affect cellular susceptibility to iAs<sup>III</sup>.

## MATERIALS AND METHODS

**Cell culture.** Human HEK293T and K562 cells lines were obtained from the biosciences divisional services cell culture facility, UC Berkeley (<https://bds.berkeley.edu/facilities/cell-culture>; Accessed February 7, 2019). HEK293T cells were cultured in Dulbecco's modified Eagles medium (DMEM; Thermo Fisher) supplemented with 10% fetal bovine serum (FBS; Corning) and 1% penicillin/streptomycin (PS; Thermo Fisher). K562 cells were cultured in RPMI 1640 (Thermo Fisher) supplemented with 10% FBS and 1% PS. Cells were cultured in a humidified incubator with 5% CO<sub>2</sub> at 37°C.

**Cytotoxicity assays.** Cell viability assays were performed using the CellTiter-Glo luminescent cell viability assay kit (Promega) following the manufacturer's protocol. In brief, cells were seeded at a density of 10<sup>5</sup> cells/ml (10<sup>4</sup> cells/well) in opaque 96-well cell culture plates. ATO/As<sub>2</sub>O<sub>3</sub> (STREM Chemicals Inc.) stock of 10 mM was prepared by dissolving 20 mg of As<sub>2</sub>O<sub>3</sub> in 300  $\mu$ l NaOH (1 M) and completing the volume to 10 ml with PBS. Cells were treated with 0, 0.5, 1, 1.5, and 2  $\mu$ M ATO for 24, 48, 72, or 96 h as indicated. For experiments involving selenium pretreatment, cells were pretreated with 10  $\mu$ M sodium selenite (Na<sub>2</sub>SeO<sub>3</sub>; MP Biomedicals) for 24 h, washed with PBS, seeded in new plates and treated with 0, 0.5, 1, 1.5, and 2  $\mu$ M ATO for 48 h. At the end of each incubation period, 100  $\mu$ l of the CellTiter Glo reagent was added to each well and the cells were lysed at an orbital plate shaker for 2 min. The plate was then incubated for 10 min at room temperature in the dark to stabilize the signal.

Luminescent signals from all wells were read on a Synergy H1 microplate reader (BioTek Instruments).

**Genome-wide and targeted CRISPR/Cas9 libraries.** The human genome-wide CRISPR knockout (GeCKO) version 2 sgRNA library cloned in LentiCRISPR v2 vector (Addgene no. 1000000048, kindly deposited by Dr Feng Zhang) was used for genome-wide screening. The GeCKO v2 library targets 19 050 protein-coding genes and 1864 miRNAs and contains 1000 nontargeting sgRNAs with a total of 123 411 sgRNAs split into 2 half libraries A and B (Sanjana et al., 2014). For primary screening, we used half library A containing 65 383 sgRNAs with an average of 3 sgRNAs targeting each gene. For the focused (validation) library, sgRNA designs targeting each selected gene were picked up from the GeCKO v2 (half-libraries A and B) and the Brunello library (Doench et al., 2016). The validation library targets 307 genes (6–8 sgRNAs/gene) and contains 500 nontargeting sgRNAs, with a total of 2784 sgRNAs. Pooled custom oligonucleotides (79 bp) comprised of the 20 bp sgRNA sequence and the appropriate upstream (5'-cttGTGGAAAGGACGAAACACCG-3') and downstream (5'-gttttagagctaGAAAtagcaagttaaaataaggct-3') flanking sequences were synthesized by CustomArray pooled oligo synthesis service (CustomArray Inc., Bothell, Waltham). The obtained full-size oligos were PCR-amplified, gel-purified and cloned into the LentiCRISPR v2 vector (Addgene no. 52961) using Gibson assembly as previously described (Shalem et al., 2014). Both GeCKO v2 and validation libraries were transformed into Endura electrocompetent cells (Lucigen) using previously described protocols for library amplification (Sanjana et al., 2014; Shalem et al., 2014). Transformation efficiency for each library ensured sufficient representation of all constructs (approximately 150-fold library size for GeCKO v2 and approximately 500-fold library size for validation library). Plasmid DNA was isolated from amplified colonies using the Maxiprep plasmid DNA purification kit (Qiagen).

**Lentiviral production and functional titration.** Lentivirus production was performed as previously described (Shalem et al., 2014), with minor modifications. Briefly, HEK293T cells cultured in a T225 flasks were co-transfected with 20  $\mu$ g of the plasmid library, 15  $\mu$ g of the packaging plasmid (psPAX2, Addgene no. 12260) and 10  $\mu$ g of the envelope plasmid (pMD2.G, Addgene no. 12259). Media containing the virus were collected 60-h posttransfection and filtered through a Steriflip-HV 0.45  $\mu$ m low protein-binding PVDF membrane (Millipore). The lentiviral supernatant was concentrated 50-fold using Lenti-X Concentrator (Clontech) following the manufacturer's protocol. Viral solutions were aliquoted and stored at –80° C until further use. To perform functional titration of the prepared viral solutions, K562 cells were suspended in transduction medium (RPMI 1640, 10% FBS, 1% PS + 8  $\mu$ g/ml polybrene) and seeded at a density of 1.25  $\times$  10<sup>6</sup> cells/ml in 12-well plates (2.5  $\times$  10<sup>6</sup> cells per well). Different volumes (0, 2.5, 5, 10, 15, and 20  $\mu$ l) of the virus were mixed with the cell suspension in each well and the plates were centrifuged at 1000 g for 2 h at 33° C. Transduced cells from each well were suspended in fresh media and recovered for 48 h. For each transduction volume, cells were seeded in 96-well plate at a density of 10<sup>5</sup> cells/ml (10<sup>4</sup> cells/well; 100  $\mu$ l) with or without puromycin (2  $\mu$ g/ml) and maintained for 7 days during which 25  $\mu$ l of cell suspension from each well were added to 75  $\mu$ l of fresh media in a new replica plate every 48 h. Following puromycin selection, cell viability in each condition was evaluated by CellTiter Glo and the multiplicity of infection (MOI) corresponding to each transduction volume was calculated by dividing the average luminescence signal from wells with puromycin

by the average luminescence signal from wells without puromycin. A transduction volume corresponding to a MOI of 0.25–0.5 was used in the large-scale transduction.

**Genome-wide (primary) screening.** GeCKO v2 library, packaged in lentiviral particles was transduced into  $100 \times 10^6$  K562 cells in 12-well plates using the same protocol described for viral titration. Each well, containing  $2.5 \times 10^6$  cells, was transduced with 10  $\mu$ l of the GeCKO v2 virus which results in a MOI of 0.45 (determined from titration). Transduced cells from all wells were pooled and the non-infected cells were eliminated by puromycin selection (2  $\mu$ g/ml) for 7 days during which the infected cells were expanded. The obtained mutant library was split into treatment (1  $\mu$ M ATO) and control (NaOH vehicle) conditions where at least  $25 \times 10^6$  cells were maintained resulting in a representation of approximately 400-fold the library size. Selection was applied for 7 days which correspond to approximately 7 K562 cell doublings and the media were replaced every 48 h. Screens were performed in T225 cell culture flasks and each condition was run in duplicate. At the end of the screen,  $25 \times 10^6$  cells from each replicate were washed with PBS and the pellets were saved for DNA extraction.

**Validation (secondary) screening.**  $10 \times 10^6$  K562 cells were transduced with the validation library in a 12-well plate using the same described protocol. Each well, containing  $2.5 \times 10^6$  cells, was transduced with 2.5  $\mu$ l of the validation library virus which results in a MOI of 0.27 (determined from titration). The same screening conditions described for the primary screen were applied for the validation screen. At least  $2.5 \times 10^6$  cells were maintained in each condition representing approximately 900-fold the library size. Screens were performed in T25 cell culture flasks and each condition was run in triplicate. At the end of the screen,  $2.5 \times 10^6$  cells from each replicate were washed with PBS and the pellets were saved for DNA extraction.

**DNA extraction, library preparation and next generation sequencing.** Genomic DNA was isolated from  $25 \times 10^6$  cells (primary screen) using the Blood and Cell Culture DNA Midi kit (Qiagen) or  $2.5 \times 10^6$  cells (secondary screen) using the DNeasy Blood and Tissue kit (Qiagen) following the manufacturer's protocols. Library preparation for next generation sequencing was performed as previously described (Sanjana et al., 2014), with minor modifications. For each sample, the pool of guide sequences was amplified from genomic DNA by high fidelity PCR using the Herculese II Fusion DNA Polymerase kit (Agilent). For the genome-wide screen, 150  $\mu$ g genomic DNA were amplified for each sample (10  $\mu$ g genomic DNA/reaction; 15 reactions/sample). For the secondary screen, 15  $\mu$ g genomic DNA were amplified for each sample (5  $\mu$ g genomic DNA/reaction; 3 reactions/sample). In addition to the appropriate amount of genomic DNA template, each PCR reaction contained 20  $\mu$ l of the 5 $\times$  reaction buffer, 500 nM of each of the forward and reverse primers, 1 mM deoxyribonucleoside triphosphates (dNTPs), 1  $\mu$ l polymerase and an appropriate volume of water to reach a final volume of 100  $\mu$ l. PCR was conducted with the following conditions: 95°C/2 min; 18 cycles of 95°C/20 s, 60°C/20 s, 72°C/30 s; followed by 72°C/3 min. Following amplification, reactions corresponding to the same sample were pooled. To prepare the samples for next generation sequencing, the obtained amplicons were further amplified using primers that include appropriate P5 and P7 illumina adapter sequences. In order to increase the diversity of the libraries, the forward primer used in the second PCR included a 5 N shuffle sequence. To allow multiplexing of

samples, multiple reverse primers were used in the second PCR and each primer contained a unique 8 bp index that was used to label each sample. For each PCR2 reaction, 5  $\mu$ l of the first PCR product were used as a template. Seven PCR2 reactions per sample were performed for the genome-wide screen while a single PCR2 reaction was performed for each sample of the validation screen. PCR2 conditions and amplification protocol were similar to those used for PCR1 but 20 amplification cycles were applied instead of 18. For the genome-wide screen, PCR2 reactions corresponding to the same sample were pooled. Primers used in the first and second PCRs are shown in Supplementary Table 1. The quality of the 358 bp PCR2 amplicon was assessed on a 2% agarose gel and then using a 2100 bioanalyzer (Agilent). If necessary, unincorporated primers and nonspecific products were removed from each sample using pippin prep (Sage Science). Following purification, individual samples labeled with different indices were quantified on a Qubit fluorometer (Thermo Fisher Scientific) and pooled in equimolar amounts. Pooled libraries were deep sequenced using the illumina Hiseq2500 platform (single read 50 bp) with a coverage exceeding 500 folds the size of each library.

**Data processing and computational analysis.** Raw FASTQ files were demultiplexed using the FASTX-Toolkit ([http://hannonlab.cshl.edu/fastx\\_toolkit/](http://hannonlab.cshl.edu/fastx_toolkit/); Accessed February 7, 2019) and processed to contain only the unique 20-bp guide sequences. To align the processed reads with the reference library, guide sequences from the library were assembled into a Burrows-Wheeler index (Li and Durbin, 2009) using the Bowtie build-index function (Langmead et al., 2009). Reads were aligned using the Bowtie aligner and the number of uniquely aligned reads (perfect match) for each guide was calculated. Individual guide counts or the sum of counts of all guides targeting each gene were used as an input into edgeR, where the counts were normalized using the upper-quartile method. Differential abundance of each guide or all guides targeting a gene between treatment and control conditions was determined using the negative binomial generalized linear model (GLM) approach implemented in edgeR (Lun et al., 2016). False discovery rates (FDRs) were estimated to correct for multiple comparisons. Primary candidate selection was based on individual guide sequences displaying differential representation between the 2 conditions with FDR < 0.1. Additional genes were identified by performing a gene-level statistical analysis, based on summing counts from all the guide sequences targeting a given gene. Validation of candidates by secondary screening was based on revealing multiple individual guide sequences per gene that are differentially represented between the 2 conditions with FDR < 0.001. A complementary gene-level confirmatory analysis was performed by fitting a separate linear model to the total sgRNA counts for each gene using the method of limma (Ritchie et al., 2015), alongside the voom transform (Law et al., 2014), implemented in the popular limma R package. Alternatively, gene ranking was performed using Model-based Analysis of Genome-wide CRISPR-Cas9 Knockout (MaGeCK), which combines ranks of individual guides targeting the same gene using a modified version of robust ranking aggregation (Li et al., 2014). Functional enrichments within the list of candidate genes were determined by gene ontology enrichment analysis implemented in the STRING database (<http://string-db.org>; Accessed February 7, 2019) complemented with literature-based manual curation.

**Generation of PSTK knockout and control pools.** sgRNAs targeting PSTK or a nontargeting (NTC) sgRNA (sequences shown in



Supplementary Table 2) were cloned into the CRISPR lentiviral backbone vector (LentiCRISPR v2) using the Golden Gate method. To produce lentiviral particles, we cotransfected HEK293T cells in T25 culture flasks with 3.4  $\mu\text{g}$  of the target vector, 2.6  $\mu\text{g}$  of the packaging plasmid (psPAX2) and 1.7  $\mu\text{g}$  of the envelope plasmid (pMD2.G) using Lipofectamine 2000 and Plus reagent (Thermo Fisher Scientific) following the manufacturer's instructions. Viral solutions were collected 60 h posttransfection, filtered through a Steriflip-HV 0.45  $\mu\text{m}$  low protein-binding PVDF membrane (Millipore), and concentrated 50 folds using Lenti-X Concentrator (Clontech) following the manufacturer's protocol. Cells were transduced with targeting or NTC vectors at a MOI < 0.5 and the transduced cells were enriched by puromycin selection. The obtained cellular pools were used in cytotoxicity assays to evaluate their sensitivity to ATO.

**Statistical analysis.** Data were presented as the mean  $\pm$  SD. Statistical significance was determined by 2-tailed, 2-sample *t* test assuming unequal variance. A *p*-value < .05 was considered statistically significant.

## RESULTS

### Genome-Wide Screen Reveals Genes Affecting Cellular Sensitivity to As<sup>III</sup>

We investigated cellular components of key mechanistic relevance to As<sup>III</sup> toxicity in K562 cells using the CRISPR-Cas9 genome-wide loss-of-function screening approach (Figure 1). We used the GeCKO v2 sgRNA library A containing 65 383 sgRNAs targeting approximately 19 000 human genes to generate a pool of K562 cells with mutations in the corresponding genes. We screened the cellular pool for mutations that alter sensitivity to a sublethal As<sup>III</sup> dose (1  $\mu\text{M}$  of ATO), inhibiting the proliferation of K562 cells by approximately 30% after 72 h, that we determined by cell viability assays (Figure 2A). At the end of the screen, differential growth of mutants between ATO treated and control (vehicle treated) pools was determined by comparing the representation of the corresponding guide sequences between the 2 pools. We selected candidate genes for further evaluation if at least one guide sequence targeting the gene demonstrated differential abundance between ATO and vehicle control at a FDR < 0.1 with average log<sub>2</sub> CPM > 2.5 (Figure 2B). Using these criteria, we identified 102 candidate genes implicated in the toxic response to As<sup>III</sup> (Supplementary Table 3). To maximize the number of candidates from the primary screen, we implemented additional analysis methods for candidate selection. An analysis approach which involves summing all guide sequences targeting the same gene identified 97 candidate genes with FDR < 0.1 (Supplementary Table 4). Among these, 49 candidates did not overlap with the list identified from the analysis approach based on individual sgRNAs (Figure 2C). Within the overlapping candidates, there were 34 genes whose disruption potentially confers resistance to As<sup>III</sup> and 14 genes whose loss potentially increases cellular sensitivity to As<sup>III</sup> (Figure 2D). A third, more stringent, analysis method using MAGeCK identified only 10 candidate genes with FDR < 0.1 (Supplementary Table 5), 9 of which were already identified by the other 2 approaches (Figure 2C).

### Simultaneous Validation of Genes Modulating As<sup>III</sup> Cytotoxicity by Secondary Screening

We generated a customized CRISPR-Cas9 validation library, with increased number of sgRNAs targeting each gene (6–8 sgRNAs/

gene), that is enriched for the primary hits identified by all the analysis methods implemented for the primary screen. We used the same validation library to confirm hits revealed by other screens which will be reported elsewhere. Thus, the validation library also included multiple sgRNAs targeting genes which were not identified as hits in the primary ATO screen in addition to several nontargeting sgRNAs. We performed a secondary screen in K562 cells with the validation library using conditions identical to those applied for the primary screen but on a smaller scale. We used more stringent criteria for candidate validation which required at least 2 sgRNAs per gene exhibiting significant depletion or enrichment in ATO compared to vehicle control with a FDR < 0.001. Using these criteria, we validated multiple primary candidates. Validated hits included genes whose loss confers either increased or decreased sensitivity to As<sup>III</sup>, with the latter being more prominent (Figure 3A; Supplementary Table 6). The secondary screen validated 20 candidates that were initially revealed by both the summing and the individual guide-based analysis methods, 16 candidates that were exclusively revealed by the summing method and 7 candidates that were uniquely identified by the individual guide-based method. Gene-level confirmatory analysis using the limma package revealed similar enrichment and depletion hits as the main GLM-based method (Supplementary Tables 8 and 9). Additionally, the vast majority of the validated genes were also revealed by MAGeCK analysis (Supplementary Tables 10 and 11). Functional classification of validated genes uncovered multiple biological processes as determinants of cellular sensitivity or tolerance to As<sup>III</sup> including selenocysteine (Sec) metabolism and utilization, oxidative stress response, DNA damage response, cellular transport, intracellular trafficking, histone modification, RNA processing in addition to diverse intracellular signaling processes (Figure 3B; Supplementary Table 7).

### Oxidative Stress Response and Certain Cellular Transporters Affect Sensitivity to As<sup>III</sup>

Disruption of KEAP1, the negative regulator of the antioxidant response transcription factor Nrf2, resulted in a striking resistance to As<sup>III</sup> (Figure 3C). Alternatively, loss of the multidrug resistance protein ABCC1 drastically increased sensitivity to As<sup>III</sup> (Figure 3D). In contrast, disruption of genes encoding other transporter proteins including aquaporin 3 (AQP3) and the zinc transporter ZnT1(SLC30A1) resulted in As<sup>III</sup> tolerance (Supplementary Table 7).

### Cellular Damage Response and DNA Repair Are Important Modulators of As<sup>III</sup> Sensitivity

Disruption of UBE2H involved in ubiquitin-dependent protein catabolism and CNOT2 involved in mRNA degradation increased sensitivity to As<sup>III</sup> (Supplementary Table 7). Multiple components of DNA damage response and double strand DNA repair were also identified in our screen (Supplementary Table 7). Unexpectedly, disruption of these genes increased resistance rather than sensitivity.

### Histone Modification, Transcriptional Regulation, and Diverse Signaling Processes Impact As<sup>III</sup> Cytotoxicity

We identified few histone-modifying factors whose disruption increased resistance to As<sup>III</sup> (Supplementary Table 7). These include MRGBP and DR1, components of the NuA4 and ATAC histone acetyltransferase complexes respectively, GFI1B, a member of several histone deacetylase complexes and EED, a member of the PRC2/EED-EZH2 complex involved in histone H3 methylation. Other transcriptional regulators whose loss

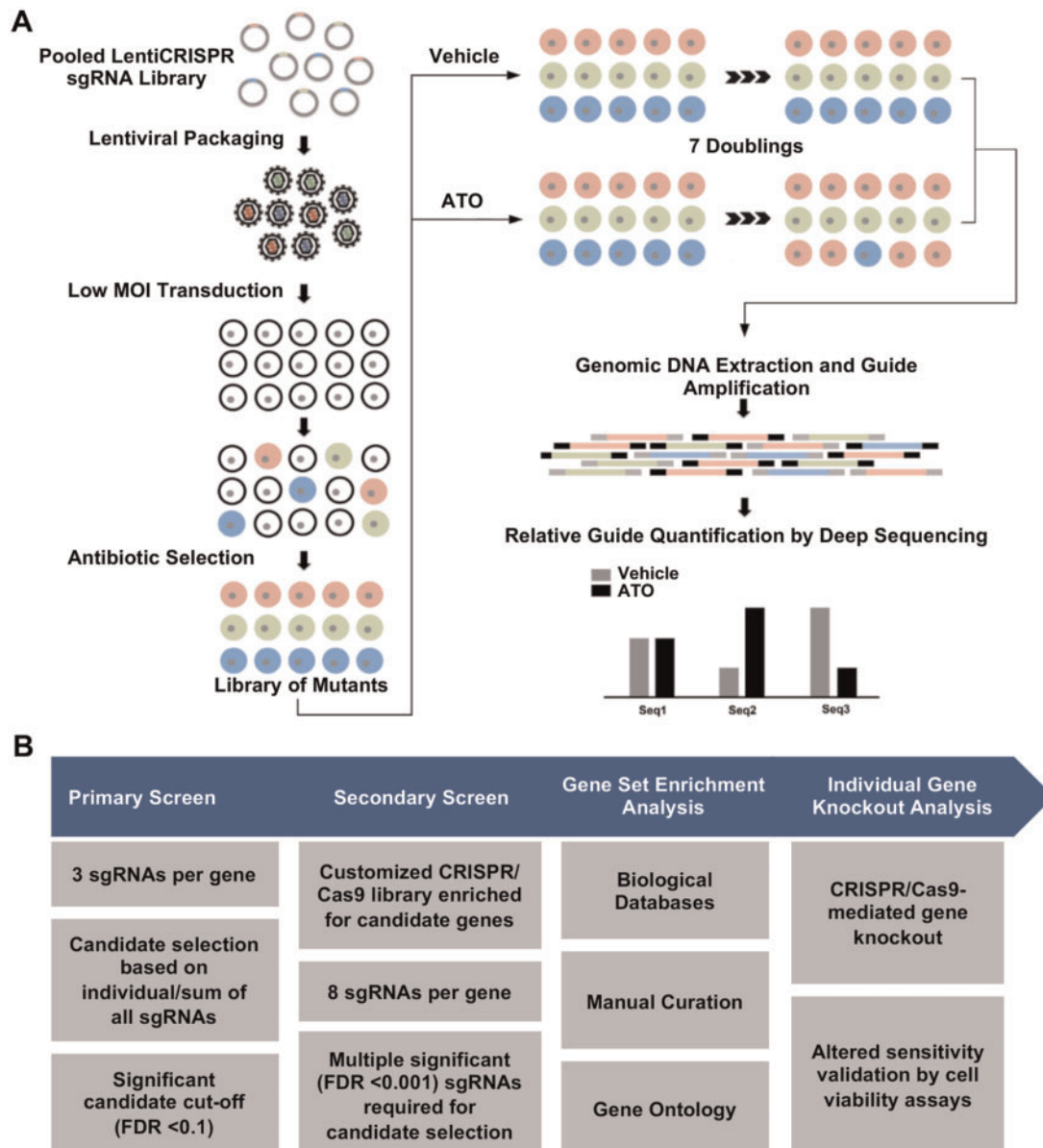


**Figure 1.** Overview of the performed CRISPR-based knockout screening approach. **A**, The Cas9-sgRNA library was packaged into lentiviral particles and transduced into K562 cells. The obtained cellular library was screened to identify mutants with growth advantage or disadvantage in the presence of ATO. Guide sequences, used as barcodes labeling the different mutants, were PCR-amplified and quantified by deep sequencing. **B**, Study workflow showing screening strategies, candidate gene selection criteria, and validation approaches.

increased As<sup>III</sup> resistance include 2 mRNA processing/splicing factors, PAPOLA and CCNL2 and 2 positive transcriptional modulators, MEIS2 and RREB1 (Supplementary Table 7). In addition, loss of intracellular signaling components such as FLCN and RRAGC involved in mechanistic target of rapamycin (mTOR) signaling, RCE1 which is required for activation of RAS signaling and CTDNEP1 which suppresses bone morphogenetic proteins (BMP) signaling resulted in As<sup>III</sup> tolerance (Supplementary Table 7).

#### Modulation of Processes Involved in Protein Translation Affects As<sup>III</sup> Cytotoxicity

Disruption of certain translation components modulated sensitivity to As<sup>III</sup> (Supplementary Table 7). Loss of 2 components of

diphthamide biosynthesis (DPH5, DPH6), a process that modifies a histidine residue in the eukaryotic translation elongation factor 2 (eEF-2), resulted in decreased sensitivity to As<sup>III</sup>. Similarly, inactivation of DHPS that uniquely modifies a specific lysine residue in eukaryotic translation initiation factor 5 A (eIF-5A) confers As<sup>III</sup> resistance.

#### Disruption of Sec Biosynthesis and Utilization Protects against As<sup>III</sup> Cytotoxicity

Inactivation of almost every gene involved in Sec biosynthesis or Sec incorporation into selenoproteins (EEFSEC, SECISBP2, SEPHS2, SEPECS, and PSTK) conferred resistance to As<sup>III</sup> (Figure 4B). At least 5 distinct sgRNAs targeting each gene, out of the 8 sgRNAs used in the secondary screen, showed significant

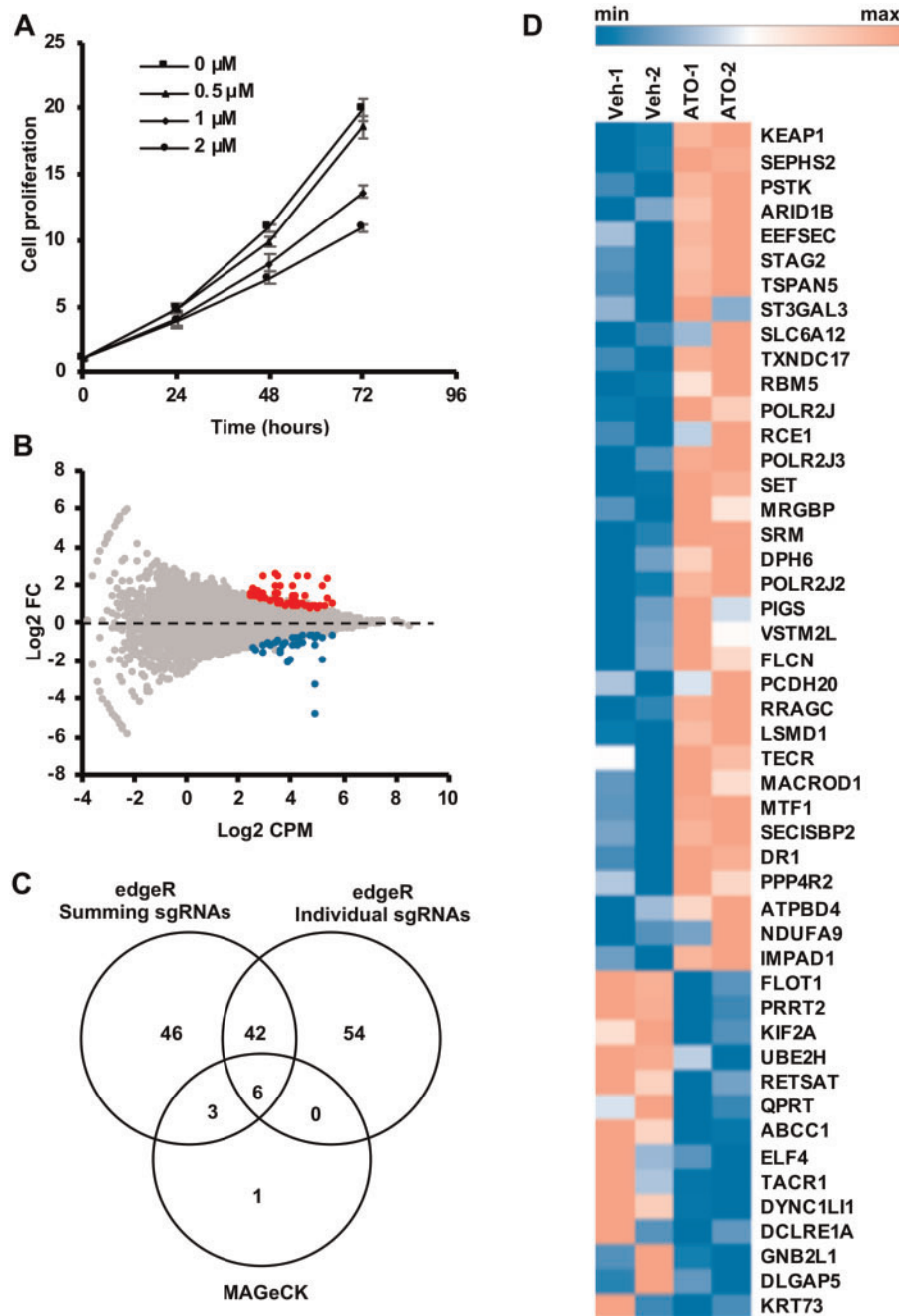


**Figure 2.** Identification of multiple candidate genes affecting ATO/As<sup>III</sup> toxicity. **A**, Cytotoxicity of multiple concentrations of ATO in K562 cells evaluated at 24, 48, and 72 h by CellTiter Glo cell proliferation assay. Data are represented as mean  $\pm$  SD ( $n = 3$ ). **B**, Scatter plot showing relative enrichment ( $\log_2$  FC  $> 0$ ) or depletion ( $\log_2$  FC  $< 0$ ) of each gene-specific guide sequence in ATO compared to vehicle control (Veh).  $\log_2$  fold changes (FC) are plotted against the average abundance of each guide sequence in the pool represented as  $\log_2$  counts per million (CPM). Hits with FDR values  $< 0.1$  are shown in different colors. **C**, Venn diagram showing unique and common candidates identified by 3 analysis methods. For each method, number of hits with FDR  $< 0.1$  is shown. **D**, Heatmap of the normalized sum of counts of all guide sequences targeting each gene. Only hits that are in common between the summing and individual sgRNA analysis approaches are shown. The screen was run in duplicate and the values corresponding to each replicate (Veh or ATO) are represented in the heat map.

enrichment in ATO relative to the vehicle control with FDRs  $< 0.001$  (Supplementary Table 6). To further confirm that Sec biosynthesis is a sensitivity determinant for As<sup>III</sup>, we targeted the phosphoserine tRNA kinase (PSTK) gene in K562 cells using the CRISPR-Cas9 knockout tool. We generated 2 independent PSTK knockout pools by transducing K562 cells with different Cas9-sgRNA vectors. Cell viability assays showed increased resistance of the PSTK mutant pools to As<sup>III</sup> (Figure 4C). Additionally,

disruption of TXNDC17 (TRP14), a substrate of the selenoprotein thioredoxin reductase (TxrR), resulted in As<sup>III</sup> tolerance (Figure 4D).

#### Selenium Enhances Tolerance of K562 Cells to As<sup>III</sup>

One potential explanation on the role of defective Sec biosynthesis/utilization in enhancing tolerance to As<sup>III</sup> is the accumulation of intracellular selenium. To study the effect of selenium

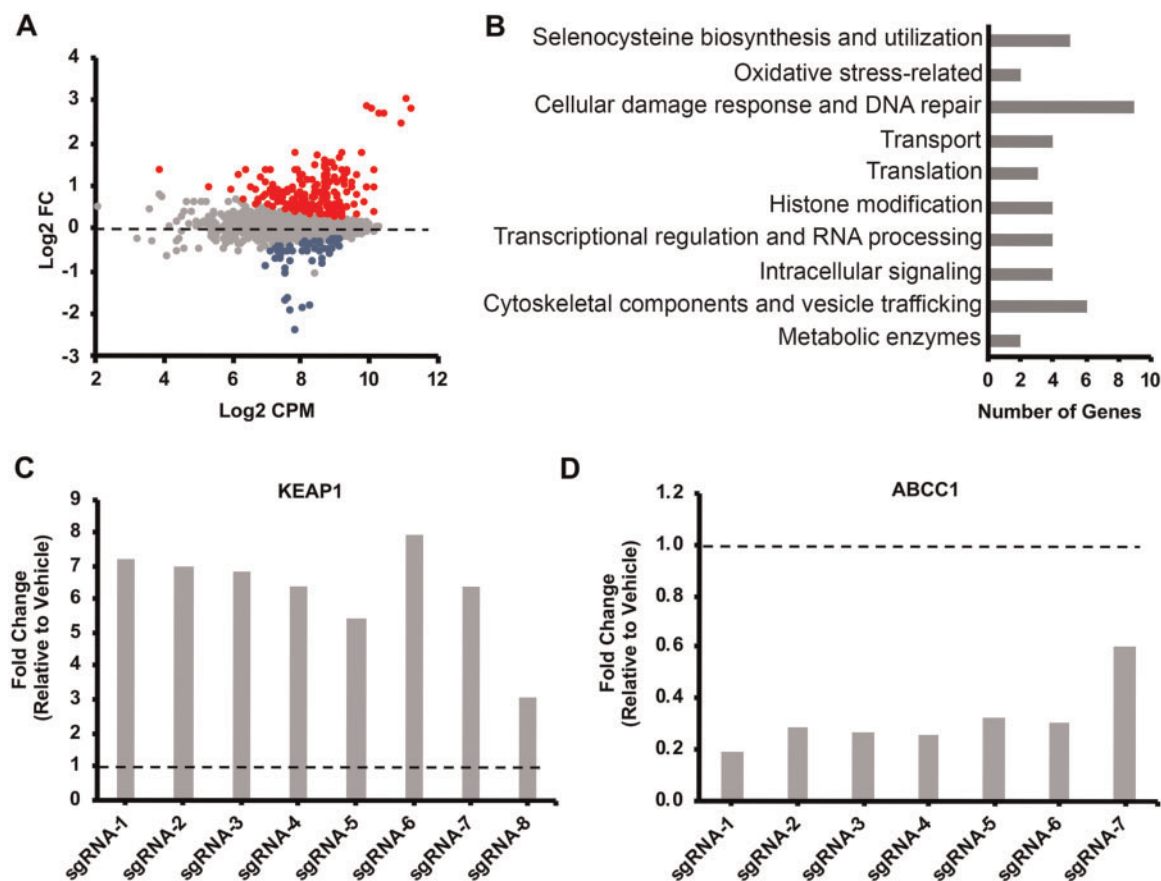


**Figure 3.** Simultaneous validation of multiple candidate genes involved in ATO/As<sup>III</sup> toxicity by secondary screening. **A**, Scatter plot showing relative enrichment ( $\log_2$  FC > 0) or depletion ( $\log_2$  FC < 0) of each gene-specific guide sequence in ATO compared to vehicle control.  $\log_2$  fold changes (FC) are plotted against the average abundance of each guide sequence in the pool represented as  $\log_2$  counts per million (CPM). Hits with FDR values < 0.001 are shown in different colors. **B**, Functional enrichment analysis of validated genes showing the top biological processes affecting ATO toxicity. Bars represent numbers of validated genes within each pathway. **C**, Relative enrichment (Fold change > 1) of each of the guide sequences targeting KEAP1 in ATO-treated compared to control pools. **D**, Relative depletion (Fold Change < 1) of each of the guide sequences targeting ABCC1 in ATO-treated compared to control pools. Fold changes for each guide sequence are calculated by dividing the normalized abundance of the sequence in ATO-treated pools by that in control pools. The dotted line ( $y = 1$ ) in each graph represents the baseline abundance of each guide sequence in control pools. Data are represented as mean ( $n = 3$ ). Only guide sequences displaying differential abundance at FDR < 0.001 are shown.

on As<sup>III</sup> toxicity in K562 cells, we pretreated cells with 10  $\mu$ M sodium selenite (Na<sub>2</sub> SeO<sub>3</sub>) as an exogenous selenium source and assessed cell viability in response to multiple As<sup>III</sup> doses. Pretreatment of cells with sodium selenite significantly improved cell viability in response to As<sup>III</sup> treatment at all the studied doses (Figure 4E).

## DISCUSSION

In this study, we used genome-wide CRISPR/Cas9 loss-of-function screening to investigate cellular mechanisms affecting susceptibility to ATO/As<sub>2</sub>O<sub>3</sub>; As<sup>III</sup> in a K562 chronic myeloid leukemia (CML) cell line. To our knowledge, this study is the first comprehensive functional investigation of the genetic components modulating the cellular toxicity of As<sup>III</sup> in mammalian cells. Inorganic As<sup>III</sup> (iAs<sup>III</sup>) can be converted intracellularly into methylated metabolites by the arsenic methyltransferase (As3MT) (Khaleghian et al., 2014). K562 cells express low levels of As3MT (Sumi et al., 2011) indicating that these cells can metabolize iAs<sup>III</sup> into the methylated forms. Diverse mechanisms of acute and chronic As<sup>III</sup> toxicity have been previously identified in whole organisms and in individual cells (Abdul et al., 2015). In addition, factors influencing susceptibility of different

individuals to arsenicals including As<sup>III</sup> were recently reviewed (Minatel et al., 2018). Our work confirmed the importance of previously well studied cellular processes, such as the oxidative stress response, in the cellular response to acute As<sup>III</sup> exposure. We also identified additional functional components and pathways whose role in cellular As<sup>III</sup> toxicity was not clearly appreciated. Both Sec production and its incorporation into selenoproteins were identified as key processes modulating As<sup>III</sup> toxicity in CML cells. Further investigation is needed to assess whether such processes define As<sup>III</sup> toxicity in other cell types. Our work further demonstrates the utility of unbiased functional screens (Gaytan and Vulpe, 2014) to identify components modulating cellular toxicity to exogenous stressors.

Our screen revealed an expected role for oxidative stress response in acute cellular toxicity of As<sup>III</sup> in K562 cells. As<sup>III</sup> induces cellular oxidative stress likely through multiple mechanisms (Flora, 2011). We found that loss of KEAP1, which negatively regulates the primary antioxidant transcription factor Nrf2, conferred substantial resistance to As<sup>III</sup> (Figure 3C). Nrf2 is responsible for the transcriptional activation of a complex antioxidant response pathway (Jaramillo and Zhang, 2013). Our finding is consistent with the reported activation of the Nrf2-KEAP1 pathway by arsenical compounds (Lau et al., 2013),



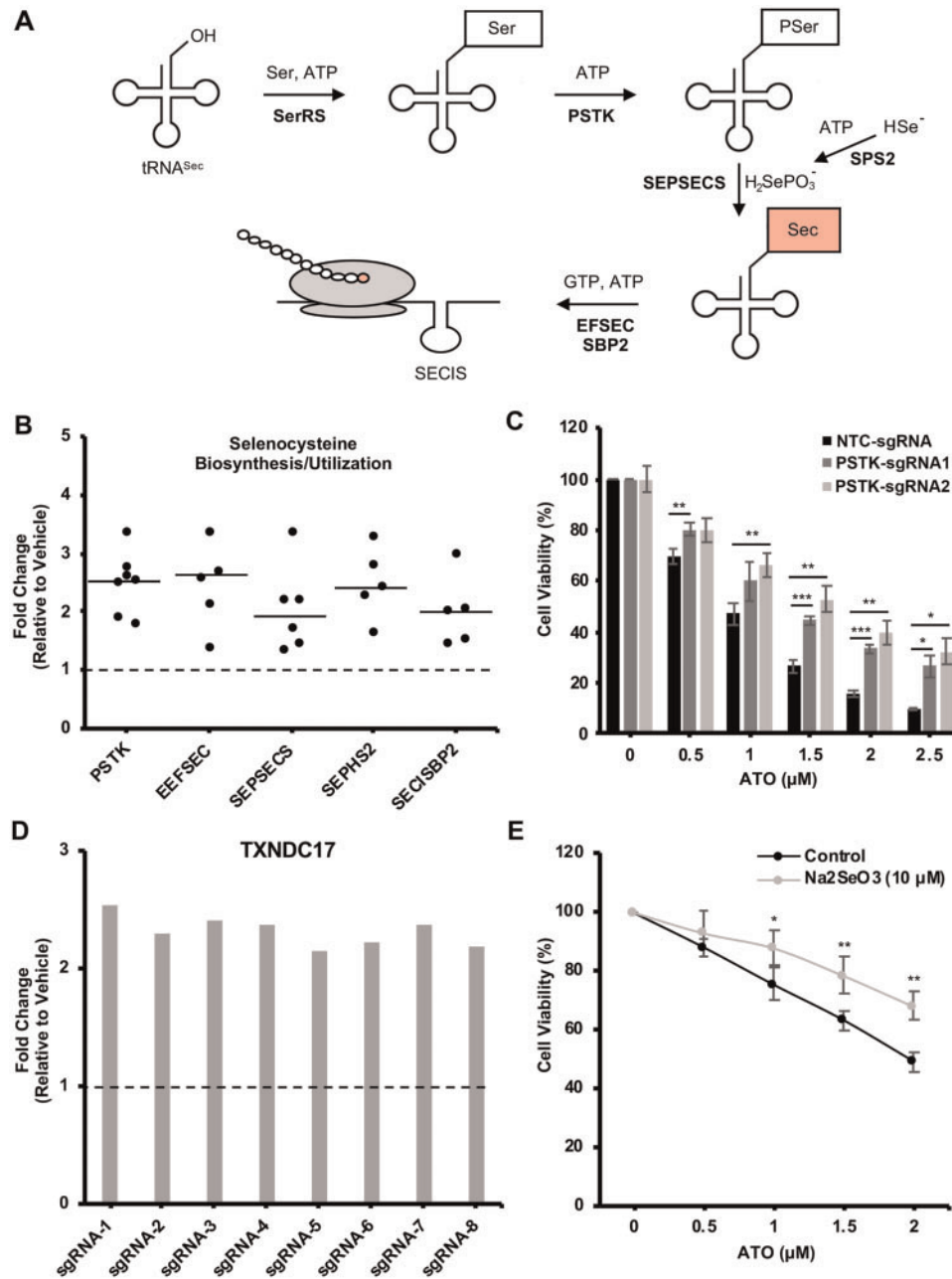


**Figure 4.** Disruption of Sec biosynthesis and utilization decreases cellular susceptibility to ATO/As<sup>III</sup>. **A**, Overview of the Sec biosynthesis pathway and incorporation into selenoproteins. **B**, Validation of the increased resistance to ATO upon disruption of genes involved in Sec biosynthesis and incorporation into proteins (obtained from secondary screening). Dots represent the different sgRNAs targeting each gene where the relative abundance of each sgRNA in the treated pools is divided by that in the control pools to calculate fold changes. The dotted line ( $y = 1$ ) represents the baseline abundance of each sgRNA sequence in control pools. Data are represented as mean ( $n = 3$ ). Only guide sequences displaying differential abundance at FDR < 0.001 are shown. Lines represent median fold enrichment of all guides corresponding to each gene. **C**, PSTK inactivation results in increased sensitivity to ATO. Cells were transduced with CRISPR/sgrNA vectors targeting PSTK or nontargeting control and treated with multiple doses of ATO for 96 h. Cell viability in each pool is shown as percentage of vehicle-treated control. Data are represented as mean of 3 independent experiments  $\pm$  SD ( $n = 3$ ). **D**, Relative enrichment (Fold Change > 1) of each of the guide sequences targeting TXNDC17 in ATO-treated compared to control pools. Fold changes for each guide sequence are calculated by dividing the normalized abundance of the sequence in ATO-treated pools by that in control pools. The dotted line ( $y = 1$ ) represents the baseline abundance of each guide sequence in control pools. Data are represented as mean ( $n = 3$ ). All the guide sequences shown display higher abundance in ATO at FDR < 0.001. **E**, Selenium protection against ATO toxicity. K562 cells were pretreated with sodium selenite (10  $\mu$ M) and ATO cytotoxicity was evaluated in pretreated and control cells at 48 h by CellTiter Glo cell viability assay. Cell viability is represented as percentage of vehicle-treated control. Data are represented as mean of 3 independent experiments  $\pm$  SD. Statistical significance was determined by Student's *t*-test, where \* $p < .05$ , \*\* $p < .01$ , \*\*\* $p < .001$ .

and the increased resistance of cells to arsenic through treatment with Nrf2 activators (Du et al., 2008). The Nrf2-KEAP1 pathway was also shown to modulate As<sup>III</sup> toxicity in NB4 APL cells (Nishimoto et al., 2016) indicating that the protective effect of

KEAP1 loss against As<sup>III</sup> is not limited to CML cells. In addition to KEAP1, we also identified TRP14 (TXNDC17), a reported reductase of L-cystine to L-cysteine in conjunction with TxrR (Pader et al., 2014), as an important determinant of As<sup>III</sup> sensitivity. L-



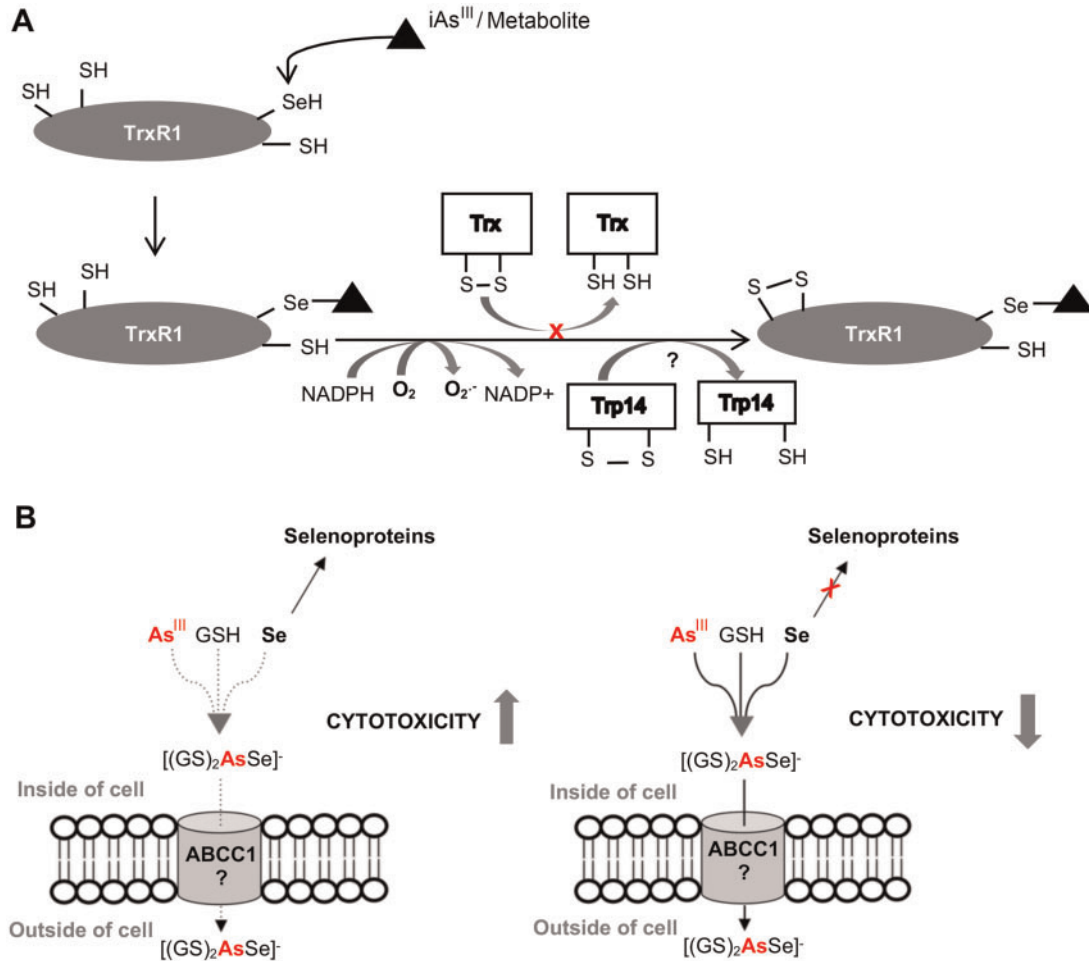


**Figure 5.** Proposed models illustrating potential roles of selenocysteine metabolism in As<sup>III</sup> toxicity. (A) Selenium Compromised Thioredoxin Reductase-derived Apoptotic Proteins (SeCTRAPS) model. Binding of inorganic As<sup>III</sup> (iAs<sup>III</sup>) or its metabolite to the selenol group of Sec in the C-terminal active site of thioredoxin reductase (TrxR1) modifies the enzyme disrupting its ability to reduce thioredoxin (Trx). The modified enzyme gains an NADPH oxidase activity that produces superoxide. TRP14, the thioredoxin-related protein encoded by the TXNDC17 gene is a potential endogenous substrate required for the NADPH oxidase activity of SeCTRAPS. (B) Seleno-bis (S-glutathionyl) arsinium ion [(GS)<sub>2</sub>AsSe]<sup>-</sup> export model. As<sup>III</sup> forms a complex with selenium and glutathione that can be exported outside the cell through multidrug resistance proteins. (Left) Utilization of selenium (Se) for selenoprotein biosynthesis may result in depletion of intracellular selenium levels and subsequent As<sup>III</sup> accumulation leading to increased cytotoxicity. (Right) Disruption of the biosynthesis of selenocysteine or its incorporation into selenoproteins can spare intracellular selenium levels resulting in efficient As<sup>III</sup> detoxification through formation of the [(GS)<sub>2</sub>AsSe]<sup>-</sup> complex and its export outside the cell.

cysteine levels are critical for GSH synthesis as well as for maintaining cytosolic GSH levels (Stipanuk *et al.*, 2006; Yu and Long, 2016). However, contrary to a role in protecting against oxidative stress via maintaining GSH levels, loss of TXNDC17, decreased rather than increased sensitivity to As<sup>III</sup> (Figure 4D) suggesting a potentially different role in As<sup>III</sup> toxicity.

Sec biosynthesis and incorporation into selenoproteins was revealed by the genome-wide CRISPR screen as a key process influencing As<sup>III</sup> toxicity in K562 CML cells. Production of Sec is initiated by charging the Sec tRNA with serine (Ser) which is converted to Sec in a multi-step process catalyzed by several enzymes (Schmidt and Simonović, 2012) (Figure 4A). Binding of the Sec tRNA (tRNA<sup>Sec</sup>) into the translational complex and subsequent insertion of Sec into the polypeptide chain requires a UGA stop codon and a downstream Sec insertion sequence (SECIS) in the corresponding mRNA and is facilitated by the SECIS-binding protein and the Sec-specific elongation factor (Hoffmann and Berry, 2006). We found that the loss of almost any enzyme involved in Sec biosynthesis or factors involved in its incorporation into the polypeptide chain results in

substantial As<sup>III</sup> tolerance (Figs. 4B and 4C). It is well-known that selenoproteins, including glutathione peroxidase and TrxR play an important role in protecting against oxidative damage (Arbogast and Ferreiro, 2010; Benhar, 2018). However, our finding that the disruption of selenoprotein synthesis increases rather than decreases tolerance to As<sup>III</sup> suggests an alternative role in As<sup>III</sup> toxicity that needs further investigation. The effect of Sec metabolism on As<sup>III</sup> toxicity could be specific to CML cells although a previous report indicated that As<sup>III</sup> can inhibit selenoprotein synthesis in A549 lung cancer cells (Talbot *et al.*, 2008). Further investigation is required to determine whether selenoprotein synthesis is a general determinant of As<sup>III</sup> cytotoxicity.

The selenoprotein, TrxR was previously identified as a direct molecular target of As<sup>III</sup> (Lu *et al.*, 2007). The Sec residue of TrxR is essential for Trx reduction as well as As<sup>III</sup> binding (Anestâl *et al.*, 2008; Lu *et al.*, 2007). Several studies indicated that binding of electrophiles, including As<sup>III</sup>, to TrxR simultaneously inhibits Trx reduction and enhances NADPH oxidase activity and thus converts the anti-oxidant protein into a pro-oxidant termed

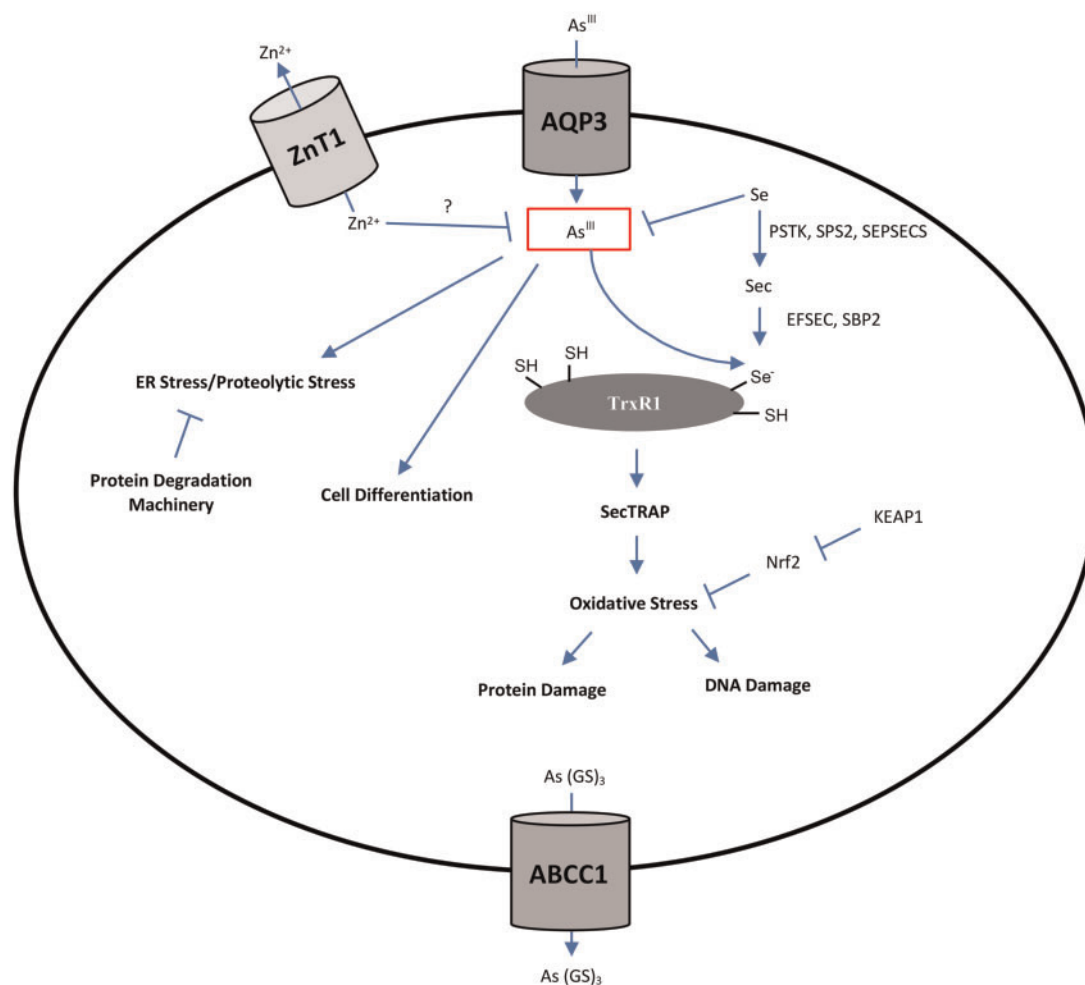


**Figure 6.** Summary of the potential cellular processes modulating As<sup>III</sup> toxicity in K562 cells revealed by CRISPR-based loss-of-function screening. As<sup>III</sup> enters the cell through Aquaporin 3 (AQP3). As<sup>III</sup> or its metabolites can have multiple cellular effects. As<sup>III</sup>-induced oxidative stress could result from mitochondrial damage and/or from a direct effect on thioredoxin reductase (TrxR) and generation of SecTRAPs. As<sup>III</sup> can have anti-proliferative effects by driving cell differentiation that is mediated by multiple cellular regulatory processes. Nrf2-based antioxidant response, intracellular selenium, intracellular zinc and export through ABCC1 can protect against As<sup>III</sup> cytotoxicity.

selenium compromised TrxR-derived apoptotic protein (SecTRAP) (Anestál and Arnér, 2003; Anestál et al., 2008) although others did not find evidence of increased NADPH oxidase activity after As<sup>III</sup> binding to TrxR *in vitro* (Lu et al., 2007). These findings, in addition to our observation that defective Sec production and insertion into selenoproteins decreases cellular sensitivity to As<sup>III</sup>, suggest that targeting of TrxR and generation of SecTRAPs could be one of the mechanisms underlying As<sup>III</sup> cytotoxicity. Therefore, resistance of Sec biosynthesis mutants to As<sup>III</sup> could be due to absence of SecTRAP formation. Additionally, it has been suggested that the apoptotic activity of the compromised TrxR requires an endogenous cellular substrate (Anestál et al., 2008). Intriguingly, the thioredoxin (Trx)-like TrxR substrate TRP14 (TXNDC17), was revealed by our screen as a determinant of sensitivity to As<sup>III</sup> (Figure 4D). This finding suggests that TRP14 could potentially serve as an endogenous substrate for SecTRAPs. The role of TRP14 in the apoptotic function of SecTRAPs requires further investigation. A proposed model for As<sup>III</sup>-derived SecTRAPs is shown in Figure 5A.

An alternative but not mutually exclusive hypothesis to explain the role of Sec biosynthesis and utilization in As<sup>III</sup>

toxicity is the reduction of intracellular selenium bioavailability. The clear interrelationship between selenite (Se<sup>IV</sup>) and As<sup>III</sup> is well documented in animals and people (Carew and Leslie, 2010; Levander, 1977; Srivastava et al., 2010; Sun et al., 2014). In mammalian cells including erythrocytes, the Selenobis (S-glutathionyl) arsinium ion ([GS]<sub>2</sub>AsSe)<sup>-</sup> can form (Manley et al., 2006) and was shown to be exported by the multidrug resistance-associated protein ABCC2 (MRP2) (Carew and Leslie, 2010). The production of Sec may reduce the bioavailable intracellular selenium pool. Thus, defective Sec biosynthesis could spare bioavailable selenium for use in the formation of the ([GS]<sub>2</sub>AsSe)<sup>-</sup> complex and hence detoxification of As<sup>III</sup> (Figure 5B). This suggestion is further supported by our finding that preloading the cells with selenium protects against subsequent As<sup>III</sup> toxicity (Figure 4E). Additionally, we identified the multidrug transporter ABCC1 (MRP1) as a major determinant of As<sup>III</sup> tolerance in K562 CML cells as its loss markedly increased As<sup>III</sup> sensitivity (Figure 3D). However, previous studies on membrane vesicles prepared from human erythrocytes indicate that ([GS]<sub>2</sub>AsSe)<sup>-</sup> complex can be exported through ABCC2 (MRP2) and not ABCC1 (Carew and Leslie, 2010). ABCC1 has been demonstrated to transport

As(GS)<sub>3</sub> complexes (Leslie, 2012; Leslie et al., 2004) so it is possible that the observed increased sensitivity upon ABCC1 loss is due to a defect in As(GS)<sub>3</sub> export rather than ([GS]<sub>2</sub>AsSe)<sup>-</sup>. Given our findings, it may be worthwhile to further investigate the role of ABCC1 in transporting ([GS]<sub>2</sub>AsSe)<sup>-</sup> in K562 cells. The role of ABCC1 in As<sup>III</sup> detoxification might be cell-type specific as its overexpression in HL60 APL cells did not result in resistance to As<sup>III</sup> (Sertel et al., 2012). Overall, our results indicate a clear relationship between intracellular Sec metabolism and cellular As<sup>III</sup> toxicity.

We identified 2 transmembrane transporters as determinants of As<sup>III</sup> sensitivity. Loss of AQP3 decreased sensitivity of K562 cells to As<sup>III</sup> consistent with a role of AQP3 in As<sup>III</sup> uptake. AQPs were previously reported to import trivalent arsenicals into mammalian cells (Rosen, 2002) and polymorphisms of AQP3 were reported to increase the risk of bladder cancer in individuals with high As<sup>III</sup> exposure (Lesseur et al., 2012). Similarly, in human lung adenocarcinoma cells, As<sup>III</sup> resistance is associated with a decrease in AQP3 expression and the knock-down of AQP3 in nonresistant cells confers As<sup>III</sup> resistance (Lee et al., 2006). Another AQP involved in As<sup>III</sup> uptake, AQP9, is not intrinsically expressed in K562 cells (Bhattacharjee et al., 2004) and hence was not identified as a modulator of As<sup>III</sup> toxicity in our screen. In contrast, the expression of AQP3 was previously detected in K562 cells (<http://www.proteinatlas.org/>; Accessed February 7, 2019). These findings indicate that multiple AQPs are involved in cellular As<sup>III</sup> uptake and that the expression of a specific AQP in a cell type defines its role in modulating As<sup>III</sup> sensitivity. We also identified the zinc exporter ZnT1 (SLC30A1) as a sensitivity factor for As<sup>III</sup> in K562 cells. Inactivation of ZnT1 or its transcriptional activator metal regulatory transcription factor 1 (MTF1) resulted in considerable As<sup>III</sup> resistance. Several groups have suggested a protective role of zinc in As<sup>III</sup> toxicity (Kreppel et al., 1994; Milton et al., 2004) which would be consistent with As<sup>III</sup> tolerance due to increased intracellular zinc levels as a result of ZnT1 dysfunction. Interestingly, SNP polymorphisms in a different zinc transporter, SLC39A2, have been associated with increased bladder cancer risk after arsenic exposure (Karagas et al., 2012).

Various cellular stress response components were identified in our study as key modulators of As<sup>III</sup> toxicity in K562 cells. For example, we found that loss of the ubiquitin conjugating enzyme UBE2H results in higher As<sup>III</sup> sensitivity suggesting a role for proteolytic stress in As<sup>III</sup> cytotoxicity. As<sup>III</sup> was previously shown to impair protein folding leading to the formation of protein aggregates in yeast (Jacobson et al., 2012). In addition, ER stress was shown to synergize with As<sup>III</sup> to induce apoptosis in APL cells (Masciarelli et al., 2018). Collectively, these findings suggest that degradation of misfolded proteins partially mitigates As<sup>III</sup> cytotoxicity. Although As<sup>III</sup> was previously shown to induce DNA damage in APL cells (Kumar et al., 2014), our results do not support a role for DNA repair in mitigating As<sup>III</sup> toxicity. We found that the disruption of selected DNA damage response and DNA repair components in K562 cells confers increased, rather than decreased, As<sup>III</sup> tolerance. It is possible that impairment of DNA damage response results in bypassing the mitotic check point, hence leading to a cellular growth advantage in the presence of As<sup>III</sup> (Bartkova et al., 2005).

Our study revealed multiple cellular processes that can modulate As<sup>III</sup> cytotoxicity (Figure 6) and hence influence its anticancer therapeutic potential. As<sup>III</sup> is a standard effective therapy for APL, and its major effects in APL cells involve the degradation of the PML-RAR $\alpha$  fusion oncoprotein (Lallemand-Breitenbach et al., 2012). However, As<sup>III</sup> can also induce

apoptosis in APL cells through other mechanisms (Davison et al., 2002; Yedjou et al., 2010). As<sup>III</sup> resistance can arise in APL leading to poor prognosis (Zhu et al., 2014). PML-RAR $\alpha$  mutations account for some but not all of the observed resistance (Chendamara et al., 2015) and our screens, although performed in CML cells, suggest potential As<sup>III</sup> resistance mechanisms that could be explored. Importantly, As<sup>III</sup> was suggested as a potential therapy for other cancer types including CML when combined with other agents such as interferons (El Eit et al., 2014) or tyrosine kinase inhibitors (Wang et al., 2015). Revealing the molecular determinants of As<sup>III</sup> sensitivity and tolerance in a CML cell line provided insight into cellular processes which can modulate the efficacy of As<sup>III</sup> in CML. Targeting such processes simultaneously with As<sup>III</sup> treatment could potentiate As<sup>III</sup> in CML therapy, with the caveat of potentially increased cytotoxicity in nontumor cells.

Our work demonstrated the capability of CRISPR-based functional genomics in deciphering molecular mechanisms modulating susceptibility to As<sup>III</sup> and our findings could have implications for a broader use of As<sup>III</sup> in chemotherapy beyond the treatment of APL. However, we recognize that the mechanisms influencing sensitivity to As<sup>III</sup> identified in K562 cells may not extend to other cell types. Hence, further studies are needed to validate the relevance of our findings in other cells and tissues. Further, additional modulators of As<sup>III</sup> sensitivity or tolerance might not have been identified by our screen due to lack of expression/activity of such determinants in K562 cells, existing compensatory mechanisms in these cells resulting in functional redundancy, or cell line specific genetic changes which abrogate the need for these modulators. Therefore, a more comprehensive approach requires complementary genetic screens in multiple cell lines to determine common as well as context-specific modulators of As<sup>III</sup> toxicity. Another limitation of our genome-wide approach could arise from poor on-target activity of the library sgRNAs which can result in false negatives. Since the genome-wide library used in our study involves only 3 sgRNAs targeting each gene, it can be expected that several determinants of As<sup>III</sup> sensitivity or tolerance in the studied cell type were not revealed. Using genome-wide libraries with improved sgRNA designs and more sgRNAs targeting each gene would likely reveal additional novel modulators of susceptibility to As<sup>III</sup>. Overall, our work is an important first step that will enable additional studies that could ultimately define all the molecular components involved in exacerbating or mitigating As<sup>III</sup> cytotoxicity.

## SUPPLEMENTARY DATA

Supplementary data are available at Toxicological Sciences online.

## DECLARATION OF CONFLICTING INTERESTS

The author(s) declared no potential conflicts of interest with respect to the research, authorship, and/or publication of this article.

## FUNDING

This work was supported by grant from the Superfund Hazardous Substance Research and Training Program (P42ES004705 to M.T.S.) and funding to C.V. from the

University of Florida Research Foundation at the University of Florida, Gainesville. A.S was a trainee in the Superfund Research Program (University of California, Berkeley). The content is solely the responsibility of the authors and does not necessarily represent the official views of the National Institute of Environmental Health Sciences.

## REFERENCES

- Abaza, Y., Kantarjian, H., Garcia-Manero, G., Estey, E., Borthakur, G., Jabbour, E., Faderl, S., O'Brien, S., Wierda, W., Pierce, S., et al. (2017). Long-term outcome of acute promyelocytic leukemia treated with all-trans-retinoic acid, arsenic trioxide, and gemtuzumab. *Blood* **129**, 1275–1283.
- Abdul, K. S., Jayasinghe, S. S., Chandana, E. P., Jayasumana, C., and De Silva, P. M. (2015). Arsenic and human health effects: A review. *Environ. Toxicol. Pharmacol.* **40**, 828–846.
- Agency for Toxic Substances and Disease Registry. (2017). Priority List of Hazardous Substances. <https://www.atsdr.cdc.gov/spl/#2017spl>. Accessed February 7, 2019.
- Akao, Y., Nakagawa, Y., and Akiyama, K. (1999). Arsenic trioxide induces apoptosis in neuroblastoma cell lines through the activation of caspase 3 in vitro. *FEBS Lett.* **455**, 59–62.
- Anestâl, K., and Arnér, E. S. J. (2003). Rapid induction of cell death by selenium-compromised thioredoxin reductase 1 but not by the fully active enzyme containing selenocysteine. *J. Biol. Chem.* **278**, 15966–15972.
- Anestâl, K., Prast-Nielsen, S., Cenas, N., and Arnér, E. S. J. (2008). Cell death by sectraps: Thioredoxin reductase as a prooxidant killer of cells. *PLoS One* **3**, e1846.
- Arbogast, S., and Ferreira, A. (2010). Selenoproteins and protection against oxidative stress: Selenoprotein n as a novel player at the crossroads of redox signaling and calcium homeostasis. *Antioxid. Redox. Signal.* **12**, 893–904.
- Bartkova, J., Horejsí, Z., Koed, K., Krämer, A., Tort, F., Zieger, K., Guldborg, P., Sehested, M., Nesland, J. M., Lukas, C., et al. (2005). DNA damage response as a candidate anti-cancer barrier in early human tumorigenesis. *Nature* **434**, 864.
- Benhar, M. (2018). Roles of mammalian glutathione peroxidase and thioredoxin reductase enzymes in the cellular response to nitrosative stress. *Free Radic. Biol. Med.* **127**, 160–164.
- Berenson, J. R., Boccia, R., Siegel, D., Bozdech, M., Bessudo, A., Stadtmayer, E., Talisman Pomeroy, J., Steis, R., Flam, M., Lutzky, J., et al. (2006). Efficacy and safety of melphalan, arsenic trioxide and ascorbic acid combination therapy in patients with relapsed or refractory multiple myeloma: A prospective, multicentre, phase ii, single-arm study. *Br. J. Haematol.* **135**, 174–183.
- Bhattacharjee, H., Carbrey, J., Rosen, B. P., and Mukhopadhyay, R. (2004). Drug uptake and pharmacological modulation of drug sensitivity in leukemia by aqp9. *Biochem. Biophys. Res. Commun.* **322**, 836–841.
- Carew, M. W., and Leslie, E. M. (2010). Selenium-dependent and -independent transport of arsenic by the human multidrug resistance protein 2 (mrp2/abcc2): Implications for the mutual detoxification of arsenic and selenium. *Carcinogenesis* **31**, 1450–1455.
- Chendamarai, E., Ganesan, S., Alex, A. A., Kamath, V., Nair, S. C., Nellickal, A. J., Janet, N. B., Srivastava, V., Lakshmi, K. M., Viswabandya, A., et al. (2015). Comparison of newly diagnosed and relapsed patients with acute promyelocytic leukemia treated with arsenic trioxide: Insight into mechanisms of resistance. *PLoS One* **10**, e0121912.
- Davison, K., Mann, K. K., and Miller, W. H. (2002). Arsenic trioxide: Mechanisms of action. *Semin. Hematol.* **39**, 3–7.
- Doench, J. G., Fusi, N., Sullender, M., Hegde, M., Vaimberg, E. W., Donovan, K. F., Smith, I., Tothova, Z., Wilen, C., Orchard, R., et al. (2016). Optimized sgRNA design to maximize activity and minimize off-target effects of CRISPR-Cas9. *Nat. Biotechnol.* **34**, 184–191.
- Du, Y., Villeneuve, N. F., Wang, X.-J., Sun, Z., Chen, W., Li, J., Lou, H., Wong, P. K., and Zhang, D. D. (2008). Oridonin confers protection against arsenic-induced toxicity through activation of the Nrf2-mediated defensive response. *Environ. Health Perspect.* **116**, 1154–1161.
- El Eit, R. M., Iskandarani, A. N., Saliba, J. L., Jabbour, M. N., Mahfouz, R. A., Bitar, N. M., Ayoubi, H. R., Zaatari, G. S., Mahon, F. X., De The, H. B., et al. (2014). Effective targeting of chronic myeloid leukemia initiating activity with the combination of arsenic trioxide and interferon alpha. *Int. J. Cancer* **134**, 988–996.
- Emadi, A., and Gore, S. D. (2010). Arsenic trioxide - an old drug rediscovered. *Blood Rev.* **24**, 191–199.
- Flora, S. J. S. (2011). Arsenic-induced oxidative stress and its reversibility. *Free Radic. Biol. Med.* **51**, 257–281.
- Gaytan, B. D., and Vulpe, C. D. (2014). Functional toxicology: Tools to advance the future of toxicity testing. *Front. Genet.* **5**, 110.
- Hoffmann, P. R., and Berry, M. J. (2006). *The Importance of Subcellular Localization of SBP2 and EFsec for Selenoprotein Synthesis*. *Selenium*, pp. 73–82. Springer, Boston, MA.
- Hopenhayn-Rich, C., Smith, A. H., and Goeden, H. M. (1993). Human studies do not support the methylation threshold hypothesis for the toxicity of inorganic arsenic. *Environ. Res.* **60**, 161–177.
- International Agency for Research on Cancer. (2004). Some Drinking-Water Disinfectants and Contaminants, Including Arsenic. IARC Monographs on the Evaluation of Carcinogenic Risks to Humans. Lyon, France: International Agency for Research on Cancer. **84**, 1–477.
- Jacobson, T., Navarrete, C., Sharma, S. K., Sideri, T. C., Ibstedt, S., Priya, S., Grant, C. M., Christen, P., Goloubinoff, P., and Tamás, M. J. (2012). Arsenite interferes with protein folding and triggers formation of protein aggregates in yeast. *J. Cell Sci.* **125**, 5073–5083.
- Jaramillo, M. C., and Zhang, D. D. (2013). The emerging role of the Nrf2-Keap1 signaling pathway in cancer. *Genes Dev.* **27**, 2179–2191.
- Karagas, M. R., Andrew, A. S., Nelson, H. H., Li, Z., Punshon, T., Schned, A., Marsit, C. J., Morris, J. S., Moore, J. H., Tyler, A. L., et al. (2012). SLC39A2 and FSIP1 polymorphisms as potential modifiers of arsenic-related bladder cancer. *Hum. Genet.* **131**, 453–461.
- Kchour, G., Tarhini, M., Kooshyar, M. M., El Hajj, H., Wattel, E., Mahmoudi, M., Hatoum, H., Rahimi, H., Maleki, M., Rafatpanah, H., et al. (2009). Phase 2 study of the efficacy and safety of the combination of arsenic trioxide, interferon alpha, and zidovudine in newly diagnosed chronic adult t-cell leukemia/lymphoma (ATL). *Blood* **113**, 6528–6532.
- Khaleghian, A., Ghaffari, S. H., Ahmadian, S., Alimoghaddam, K., and Ghavamzadeh, A. (2014). Metabolism of arsenic trioxide in acute promyelocytic leukemia cells. *J. Cell Biochem.* **115**, 1729–1739.
- Kreppel, H., Liu, J., Liu, Y., Reichl, F. X., and Klaassen, C. D. (1994). Zinc-induced arsenite tolerance in mice. *Toxicol. Sci.* **23**, 32–37.



- Kumar, S., Yedjou, C. G., and Tchounwou, P. B. (2014). Arsenic trioxide induces oxidative stress, DNA damage, and mitochondrial pathway of apoptosis in human leukemia (hl-60) cells. *J. Exp. Clin. Cancer Res.* **33**, 42.
- Lallemant-Breitenbach, V., Zhu, J., Chen, Z., and de Thé, H. (2012). Curing APL through PML/RARA degradation by As<sub>2</sub>O<sub>3</sub>. *Trends Mol. Med.* **18**, 36–42.
- Langmead, B., Trapnell, C., Pop, M., and Salzberg, S. L. (2009). Ultrafast and memory-efficient alignment of short DNA sequences to the human genome. *Genome Biol.* **10**, R25.
- Lau, A., Whitman, S. A., Jaramillo, M. C., and Zhang, D. D. (2013). Arsenic-mediated activation of the nrf2-keap1 antioxidant pathway. *J. Biochem. Mol. Toxicol.* **27**, 99–105.
- Law, C. W., Chen, Y., Shi, W., and Smyth, G. K. (2014). Voom: Precision weights unlock linear model analysis tools for RNA-seq read counts. *Genome Biol.* **15**, R29.
- Lee, T.-C., Ho, I. C., Lu, W.-J., and Huang, J.-d. (2006). Enhanced expression of multidrug resistance-associated protein 2 and reduced expression of aquaglyceroporin 3 in an arsenic-resistant human cell line. *J. Biol. Chem.* **281**, 18401–18407.
- Leslie, E. M. (2012). Arsenic–glutathione conjugate transport by the human multidrug resistance proteins (MRPs/ABCCs). *J. Inorg. Biochem.* **108**, 141–149.
- Leslie, E. M., Haimeur, A., and Waalkes, M. P. (2004). Arsenic transport by the human multidrug resistance protein 1 (MRP1/ABCC1). Evidence that a tri-glutathione conjugate is required. *J. Biol. Chem.* **279**, 32700–32708.
- Lesseur, C., Gilbert-Diamond, D., Andrew, A. S., Ekstrom, R. M., Li, Z., Kelsey, K. T., Marsit, C. J., and Karagas, M. R. (2012). A case-control study of polymorphisms in xenobiotic and arsenic metabolism genes and arsenic-related bladder cancer in New Hampshire. *Toxicol. Lett.* **210**, 100–106.
- Levander, O. A. (1977). Metabolic interrelationships between arsenic and selenium. *Environ. Health Perspect.* **19**, 159–164.
- Li, H., and Durbin, R. (2009). Fast and accurate short read alignment with burrows-wheeler transform. *Bioinformatics* **25**, 1754–1760.
- Li, W., Xu, H., Xiao, T., Cong, L., Love, M. I., Zhang, F., Irizarry, R. A., Liu, J. S., Brown, M., and Liu, X. S. (2014). Mageck enables robust identification of essential genes from genome-scale CRISPR/Cas9 knockout screens. *Genome Biol.* **5**, 554.
- Lo-Coco, F., Di Donato, L., Gimema, Schlenk, R. F., German-Austrian, A. M., Leukemia, S. G., and Study, A. L. (2016). Targeted therapy alone for acute promyelocytic leukemia. *N. Engl. J. Med.* **374**, 1197–1198.
- Lu, J., Chew, E.-H., and Holmgren, A. (2007). Targeting thioredoxin reductase is a basis for cancer therapy by arsenic trioxide. *Proc. Natl. Acad. Sci. U.S.A.* **104**, 12288–12293.
- Lun, A. T., Chen, Y., and Smyth, G. K. (2016). It's DE-licious: A recipe for differential expression analyses of RNA-seq experiments using quasi-likelihood methods in edgeR. *Methods Mol. Biol.* **1418**, 391–416.
- Manley, S. A., George, G. N., Pickering, I. J., Glass, R. S., Prenner, E. J., Yamdagni, R., Wu, Q., and Gailer, J. (2006). The seleno bis(s-glutathionyl) arsinium ion is assembled in erythrocyte lysate. *Chem. Res. Toxicol.* **19**, 601–607.
- Masciarelli, S., Capuano, E., Ottone, T., Divona, M., De Panfilis, S., Banella, C., Noguera, N. I., Picardi, A., Fontemaggi, G., Blandino, G., et al. (2018). Retinoic acid and arsenic trioxide sensitize acute promyelocytic leukemia cells to ER stress. *Leukemia* **32**, 285–294.
- Mass, M. J., Tennant, A., Roop, B. C., Cullen, W. R., Styblo, M., Thomas, D. J., and Kligerman, A. D. (2001). Methylated trivalent arsenic species are genotoxic. *Chem. Res. Toxicol.* **14**, 355–361.
- Mathews, V., George, B., Chendamarai, E., Lakshmi, K. M., Desire, S., Balasubramanian, P., Viswabandya, A., Thirugnanam, R., Abraham, A., Shaji, R. V., et al. (2010). Single-agent arsenic trioxide in the treatment of newly diagnosed acute promyelocytic leukemia: Long-term follow-up data. *J. Clin. Oncol.* **28**, 3866–3871.
- Mathews, V., George, B., Lakshmi, K. M., Viswabandya, A., Bajel, A., Balasubramanian, P., Shaji, R. V., Srivastava, V. M., Srivastava, A., and Chandy, M. (2006). Single-agent arsenic trioxide in the treatment of newly diagnosed acute promyelocytic leukemia: Durable remissions with minimal toxicity. *Blood* **107**, 2627–2632.
- Miller, W. H., Schipper, H. M., Lee, J. S., Singer, J., and Waxman, S. (2002). Mechanisms of action of arsenic trioxide. *Cancer Res.* **62**, 3893–3903.
- Milton, A. G., Zalewski, P. D., and Ratnaike, R. N. (2004). Zinc protects against arsenic-induced apoptosis in a neuronal cell line, measured by DEVD-caspase activity. *Biometals* **17**, 707–713.
- Minatel, B. C., Sage, A. P., Anderson, C., Hubaux, R., Marshall, E. A., Lam, W. L., and Martinez, V. D. (2018). Environmental arsenic exposure: From genetic susceptibility to pathogenesis. *Environ. Int.* **112**, 183–197.
- Nishimoto, S., Suzuki, T., Koike, S., Yuan, B., Takagi, N., and Ogasawara, Y. (2016). Nrf2 activation ameliorates cytotoxic effects of arsenic trioxide in acute promyelocytic leukemia cells through increased glutathione levels and arsenic efflux from cells. *Toxicol. Appl. Pharmacol.* **305**, 161–168.
- Pader, I., Sengupta, R., Cebula, M., Xu, J., Lundberg, J. O., Holmgren, A., Johansson, K., and Arnér, E. S. J. (2014). Thioredoxin-related protein of 14 kda is an efficient l-cystine reductase and S-denitrosylase. *Proc. Natl. Acad. Sci. U.S.A.* **111**, 6964–6969.
- Ratnaike, R. (2003). Acute and chronic arsenic toxicity. *Postgrad. Med. J.* **79**, 391–396.
- Ravenscroft P. (2007). Predicting the global distribution of natural arsenic pollution in groundwater. Royal Geographical Society Annual International Conference. [https://www.geog.cam.ac.uk/research/projects/arsenic/symposium/S1.2\\_P\\_Ravenscroft.pdf](https://www.geog.cam.ac.uk/research/projects/arsenic/symposium/S1.2_P_Ravenscroft.pdf). Accessed February 7, 2019.
- Ritchie, M. E., Phipson, B., Wu, D., Hu, Y., Law, C. W., Shi, W., and Smyth, G. K. (2015). Limma powers differential expression analyses for RNA-sequencing and microarray studies. *Nucleic Acids Res.* **43**, e47.
- Rosen, B. P. (2002). Biochemistry of arsenic detoxification. *FEBS Lett.* **529**, 86–92.
- Rousselot, P., Labaume, S., Marolleau, J. P., Larghero, J., Noguera, M. H., Brouet, J. C., and Feraud, J. P. (1999). Arsenic trioxide and melarsoprol induce apoptosis in plasma cell lines and in plasma cells from myeloma patients. *Cancer Res.* **59**, 1041–1048.
- Sanjana, N. E., Shalem, O., and Zhang, F. (2014). Improved vectors and genome-wide libraries for CRISPR screening. *Nat. Methods* **11**, 783–784.
- Schmidt, R. L., and Simonović, M. (2012). Synthesis and decoding of selenocysteine and human health. *Croat. Med. J.* **53**, 535–550.
- Sertel, S., Tome, M., Briehl, M. M., Bauer, J., Hock, K., Plinkert, P. K., and Efferth, T. (2012). Factors determining sensitivity and resistance of tumor cells to arsenic trioxide. *PLoS One* **7**, e35584.

- Shalem, O., Sanjana, N. E., Hartenian, E., Shi, X., Scott, D. A., Mikkelsen, T. S., Heckl, D., Ebert, B. L., Root, D. E., Doench, J. G., et al. (2014). Genome-scale CRISPR-Cas9 knockout screening in human cells. *Science* **343**, 84–87.
- Shen, Z. X., Chen, G. Q., Ni, J. H., Li, X. S., Xiong, S. M., Qiu, Q. Y., Zhu, J., Tang, W., Sun, G. L., Yang, K. Q., et al. (1997). Use of arsenic trioxide (As<sub>2</sub>O<sub>3</sub>) in the treatment of acute promyelocytic leukemia (apl): II. Clinical efficacy and pharmacokinetics in relapsed patients. *Blood* **89**, 3354–3360.
- Shen, Z. Y., Tan, L. J., Cai, W. J., Shen, J., Chen, C., Tang, X. M., and Zheng, M. H. (1999). Arsenic trioxide induces apoptosis of oesophageal carcinoma in vitro. *Int. J. Mol. Med.* **4**, 33–37.
- Srivastava, D., Subramanian, R. B., Madamwar, D., and Flora, S. J. S. (2010). Protective effects of selenium, calcium, and magnesium against arsenic-induced oxidative stress in male rats. *Arh. Hig. Rada Toksikol.* **61**, 153–159.
- Stipanuk, M. H., Dominy, J. J. E., Lee, J.-I., and Coloso, R. M. (2006). Mammalian cysteine metabolism: New insights into regulation of cysteine metabolism. *J. Nutr.* **136**, 1652S–1659S.
- Styblo, M., Drobna, Z., Jaspers, I., Lin, S., and Thomas, D. J. (2002). The role of biomethylation in toxicity and carcinogenicity of arsenic: A research update. *Environ. Health Perspect* **110**(Suppl 5), 767–771.
- Sumi, D., Fukushima, K., Miyataka, H., and Himeno, S. (2011). Alternative splicing variants of human arsenic (+3 oxidation state) methyltransferase. *Biochem. Biophys. Res. Commun.* **415**, 48–53.
- Sun, H. J., Rathinasabapathi, B., Wu, B., Luo, J., Pu, L. P., and Ma, L. Q. (2014). Arsenic and selenium toxicity and their interactive effects in humans. *Environ. Int.* **69**, 148–158.
- Talbot, S., Nelson, R., and Self, W. (2008). Arsenic trioxide and auranofin inhibit selenoprotein synthesis: Implications for chemotherapy for acute promyelocytic leukaemia. *Br. J. Pharmacol.* **154**, 940–948.
- Vahter, M. (2002). Mechanisms of arsenic biotransformation. *Toxicology* **181–182**, 211–217.
- Wang, W., Lv, F. F., Du, Y., Li, N., Chen, Y., and Chen, L. (2015). The effect of nilotinib plus arsenic trioxide on the proliferation and differentiation of primary leukemic cells from patients with chronic myeloid leukemia in blast crisis. *Cancer Cell Int.* **15**, 10.
- Watson WH. (2015). Chapter two - molecular mechanisms in arsenic toxicity. In: Fishbein JC, Heilman JM, editors. *Advances in molecular toxicology*. Waltham, MA: Elsevier. p. 35–75.
- World Health Organization & International Program on Chemical Safety. (1996). *Guidelines for drinking-water quality*. Vol. 2, Health criteria and other supporting information, 2nd ed. Geneva: World Health Organization. <https://apps.who.int/iris/handle/10665/38551>. Accessed February 7, 2019.
- Yedjou, C., Tchounwou, P., Jenkins, J., and McMurray, R. (2010). Basic mechanisms of arsenic trioxide (ato)-induced apoptosis in human leukemia (hl-60) cells. *J. Hematol. Oncol.* **3**, 28.
- Yu, X., and Long, Y. C. (2016). Crosstalk between cystine and glutathione is critical for the regulation of amino acid signaling pathways and ferroptosis. *Sci. Rep.* **6**, 30033.
- Zhang, W., Ohnishi, K., Shigeno, K., Fujisawa, S., Naito, K., Nakamura, S., Takeshita, K., Takeshita, A., and Ohno, R. (1998). The induction of apoptosis and cell cycle arrest by arsenic trioxide in lymphoid neoplasms. *Leukemia* **12**, 1383–1391.
- Zhang, X. W., Yan, X. J., Zhou, Z. R., Yang, F. F., Wu, Z. Y., Sun, H. B., Liang, W. X., Song, A. X., Lallemand-Breitenbach, V., Jeanne, M., et al. (2010). Arsenic trioxide controls the fate of the pml-raralpha oncoprotein by directly binding pml. *Science* **328**, 240–243.
- Zheng, W. L., Zhang, G. S., Xu, Y. X., Shen, J. K., Dai, C. W., and Pei, M. F. (2008). Arsenic trioxide, thalidomide and retinoid acid combination therapy in higher risk myelodysplastic syndrome patients. *Leuk. Res.* **32**, 251–254.
- Zhou, J., Zhang, Y., Li, J., Li, X., Hou, J., Zhao, Y., Liu, X., Han, X., Hu, L., Wang, S., et al., (2010). Single-agent arsenic trioxide in the treatment of children with newly diagnosed acute promyelocytic leukemia. *Blood* **115**, 1697–1702.
- Zhu, H.-H., Qin, Y.-Z., and Huang, X.-J. (2014). Resistance to arsenic therapy in acute promyelocytic leukemia. *N. Engl. J. Med.* **370**, 1864–1866.